Tetrahedron 64 (2008) 5692–5698

Contents lists available at ScienceDirect

Tetrahedron

journal homepage: www.elsevier.com/locate/tet

Distribution of photo-cross-linked products from 3-aryl-3-trifluoromethyldiazirines and alcohols

Naoki Kanoh [a,b,*,†], Takemichi Nakamura [c,*,†], Kaori Honda [a], Hiroyuki Yamakoshi [b], Yoshiharu Iwabuchi [b], Hiroyuki Osada [a]

[a] Antibiotics Laboratory, Advanced Science Institute, RIKEN, 2-1 Hirosawa, Wako, Saitama 351-0198, Japan
[b] Graduate School of Pharmaceutical Sciences, Tohoku University, Aobayama, Sendai 980-8578, Japan
[c] Molecular Characterization Team, Advanced Science Institute, RIKEN, 2-1 Hirosawa, Wako, Saitama 351-0198, Japan

ARTICLE INFO

Article history:
Received 5 February 2008
Received in revised form 8 April 2008
Accepted 8 April 2008
Available online 11 April 2008

ABSTRACT

The photolysis of *N*-[4-(3-trifluoromethyl-3*H*-diazirin-3-yl)benzoyl]-2,2′-ethylenedioxybis(ethylamine) (**1**) in EtOH, PrOH, *i*-PrOH, BuOH, and *i*-BuOH was carried out in both solution (at room temperature) and solid phase (at −196 °C), and the resultant C–H and O–H insertion products were analyzed semi-quantitatively by LC/ESI-MS/MS. The carbene insertion reactions at low temperature produced all possible C–H and O–H insertion products in a relatively uniform distribution, which could not be accomplished by the solution-phase reaction.

© 2008 Elsevier Ltd. All rights reserved.

1. Introduction

3-Aryl-3-trifluoromethyldiazirines have been used primarily in photoaffinity labeling, a biochemical approach to identify a specific receptor for a small-molecule ligand and a binding site within the receptor molecule.[1] Upon UV irradiation, the photoreactive group introduced into the ligand is promoted to a carbene, which in turn binds irreversibly to the receptor at the interaction site. Photo-generated carbenes are very reactive and are thought to have a low functional-group selectivity, which makes them essentially useless for conventional organic synthesis, but recently it has been suggested that they may have many applications in chemical biology. For example, Richards et al.[2] and Delfino et al.[3,4] have used methylene carbene as a probing agent for protein surfaces, structures, and folding. We and others have utilized carbenes generated from immobilized aryldiazirines to photo-cross-link small molecules onto solid surfaces as microarrays[5–8] and affinity beads (Fig. 1a).[9,10] These platforms are useful for screening protein–small molecule interactions.

The photo-cross-linking strategy for immobilizing small molecules onto a solid surface is unique in terms of attachment site selectivity. We have shown that a carbene photo-generated from *N*-[4-(3-trifluoromethyl-3*H*-diazirin-3-yl)benzoyl]-2,2′-ethylenedioxybis(ethylamine) (**1**) not only reacted and was introduced into a variety of small molecules[5,6] but also generated multiple conjugates from a molecule.[7] The latter is very important to detect possible binding proteins for small molecules because there are examples in which one small molecule interacts with multiple proteins by using different areas of its surface.[11,12] To maximize cross-linking efficiency and randomness toward functional groups, we carry out the photo-cross-linking reaction in a semi-solid and highly concentrated state (Fig. 1a):[13] for example, when we prepare microarrays, each small molecule solution spotted as an array was dried and concentrated on the solid surface prior to photolysis. Upon photolysis, the reactive carbene and a proximal small molecule (or a functional group), which usually diffuse away in a fluid solution, are expected not to diffuse apart because of limited diffusibility. Therefore, even a small molecule (or a functional group) having low reactivity would react efficiently with a proximal carbene to give a conjugate.[8] Unless the small molecule and carbene are aligned regularly, the cross-linking reaction occurs with low functional group selectivity. To the best of our knowledge, there is no precedent for producing a variety of surface-immobilized conjugates from a small molecule.[14]

However, to explore the scope and limitations of the photo-cross-linked platforms, it is important to know what functional groups on a small molecule are used to produce conjugates with photo-generated carbenes and to what extent these reactions proceed.

In 1970s and 1980s, groups led by Tomioka, Plats, Moss, and Gaspar studied the reactivity of photo-generated aryl carbenes extensively. The carbenes were mostly derived from parent diazo compounds in solidified organic molecules.[15,16] Relatively few

* Corresponding authors. Tel./fax: +81 22 795 6847 (N.K.); tel.: +81 48 467 9364; fax: +81 48 467 4629 (T.N.).
E-mail addresses: kanoh@mail.pharm.tohoku.ac.jp (N. Kanoh), takemi@postman.riken.go.jp (T. Nakamura).
† Contributed equally to this work.

0040-4020/$ – see front matter © 2008 Elsevier Ltd. All rights reserved.
doi:10.1016/j.tet.2008.04.031

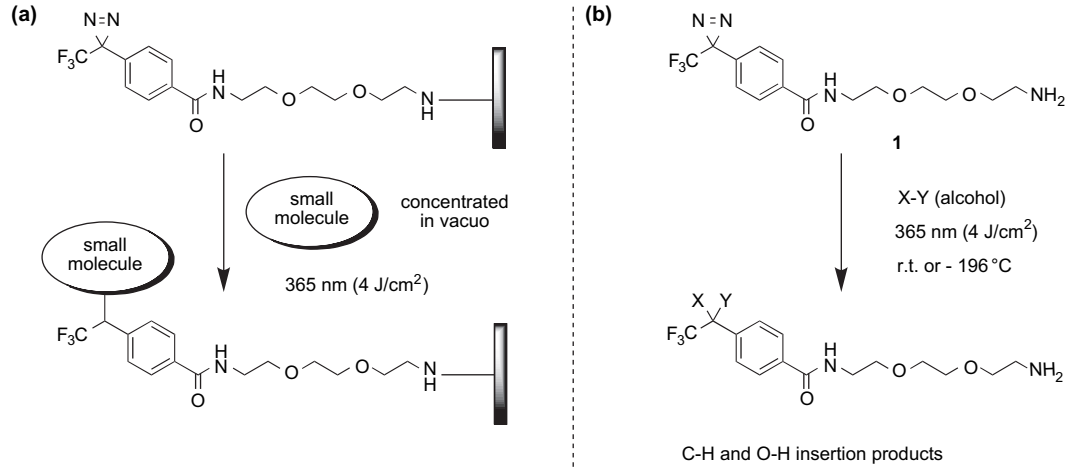

Figure 1. Production of photoadducts.

studies have provided detailed and quantitative data regarding the selectivity of diazirine-derived carbenes, particularly those, which are linked to the other structures such as fatty acyl chains and peptides.[17–21] Specifically, information on the reactivity of photo-generated carbenes from **1** would be very important for us in the development of photo-cross-linked platforms. However, to analyze the structures of the multiple conjugates generated from the photo-cross-linking reaction, sensitive and systematic methods are needed.

Toward these ends, we have initiated studies to analyze and quantify the functional-group selectivity of photo-generated carbenes from **1**. As preliminary results from these efforts, we describe the semi-quantitative and systematic analysis of photolysis products of **1** in alcohols at ambient and low temperatures by LC/ESI-MS/MS and MS/MS/MS (Fig. 1b).

2. Results and discussions

2.1. Photolysis of 1 in EtOH: characterization of all reaction products and observation of dramatic differences in product distribution depending on the reaction state (i.e., reaction temperature)

The photolysis of aryldiazirines in organic solvents has been reported to produce a variety of products.[18–20,22] Indeed, as shown in Figure 2a and b, we observed eight new peaks (**2**–**10**) after irradiation (365 nm, 4 J/cm^2) of an EtOH solution of **1** (~2 mM) at room temperature. Among those eight products, three compounds (**3**, **6**, and **8**; shaded peaks in Fig. 2b) were each shown by LC/ESI-MS to have a molecular weight of 378 (observed as MH^+: *m*/*z* 379), which was expected when the photo-generated carbene was inserted into an EtOH molecule. The structures of the EtOH adducts **3**, **6**, and **8** were identified as ethyl ether and two diastereomers of secondary alcohols as shown in Figure 2d, respectively.[23]

Structures of the other products were also elucidated. Compound **2** was found to be identical to **1** in molecular weight but to have a different retention time in LC. The UV spectrum of **2** revealed that the compound has an absorption maximum at 293 nm, suggesting that it was a diazo isomer as shown in Figure 2d.[24] Compounds **7** and **10** were found to have the same molecular weight of 366 (MH^+: *m*/*z* 367), corresponding to formal adducts between the photo-generated carbene and H_2O_2. Because peak **7** disappeared when triphenylphosphine was added to the reaction mixture after irradiation, we assigned compound **7** as a hydroperoxide. Compound **10** was identified as a hydrate of aryl trifluoromethyl ketone **11**.[23] Compounds **7** and **11** would have been generated by the reaction of the carbene and dissolved oxygen.[25] Compounds **4** (MH^+: *m*/*z* 335) and **9** (MH^+: *m*/*z* 351) were identified as a formally reduced product and a formal H_2O adduct, respectively.[23]

The same reaction performed at −196 °C, i.e., in the solid state, gave almost the same products but with significantly different product distributions. As clearly shown in Figure 2c, the carbene insertion reaction with ethanol predominated over the other type of reaction in the solid state: the ratio of the EtOH adducts (shaded peaks) increased dramatically. In addition, MS/MS experiments revealed that a large peak at ~33 min contained two products: primary alcohol **5**[23] and the secondary alcohol **6**.

The product distribution of the EtOH adducts was estimated on the basis of the total ion chromatogram generated from the MS data set for *m*/*z* 379. The relative ratios of peak intensities derived from each compound were highly reproducible. Estimation using a UV chromatogram was another possibility, but it was difficult to deduce the distribution from the UV trace because of signal overlap and a lack of sensitivity. In the case of the overlapping of cross-linked products in the chromatogram (for example, compounds **5** and **6**), we estimated that diastereomers having the same atom connectivity should be generated as a 1:1 mixture. This estimation is thought to be acceptable because most pairs of diastereomers throughout in this study were found to be produced approximately in a 1:1 ratio when good peak separation was observed (vide infra). As a result, the product distributions of EtOH adducts (**3**/**5**/**6**/**8**) were estimated to be 87:0:6:7[26] and 21:13:33:33 in the liquid and solid states, respectively.

2.2. MS fragmentation pattern analysis of the EtOH adducts

The collision-induced dissociation (CID) MS/MS spectra of compounds **3**, **5**, **6**, and **8** are shown in Figure 3a–d. The fragmentation patterns of the structural isomers were clearly different, whereas those of the diastereomers (**6** and **8**) were almost identical. The major product ions in the CID spectrum of each structural isomer were assigned as shown in Figure 3e–g on the basis of MS/MS and MS/MS/MS experiments, accurate mass measurements, and deuterium-labeling experiments.

Two primary fragmentation pathways that give *m*/*z* 274 and 231 were dominant in the CID mass spectrum of compound **3** (Fig. 3a). The product ion at *m*/*z* 176 may be generated by a secondary fragmentation from *m*/*z* 274, i.e., losses of CF_3 and C_2H_5 from the product ion at *m*/*z* 274 (Fig. 3e). In contrast to this, different secondary fragmentation pathways that give *m*/*z* 211 and 213, i.e., a loss of HF or H_2O from *m*/*z* 231, emerged in the CID spectrum of **5**,

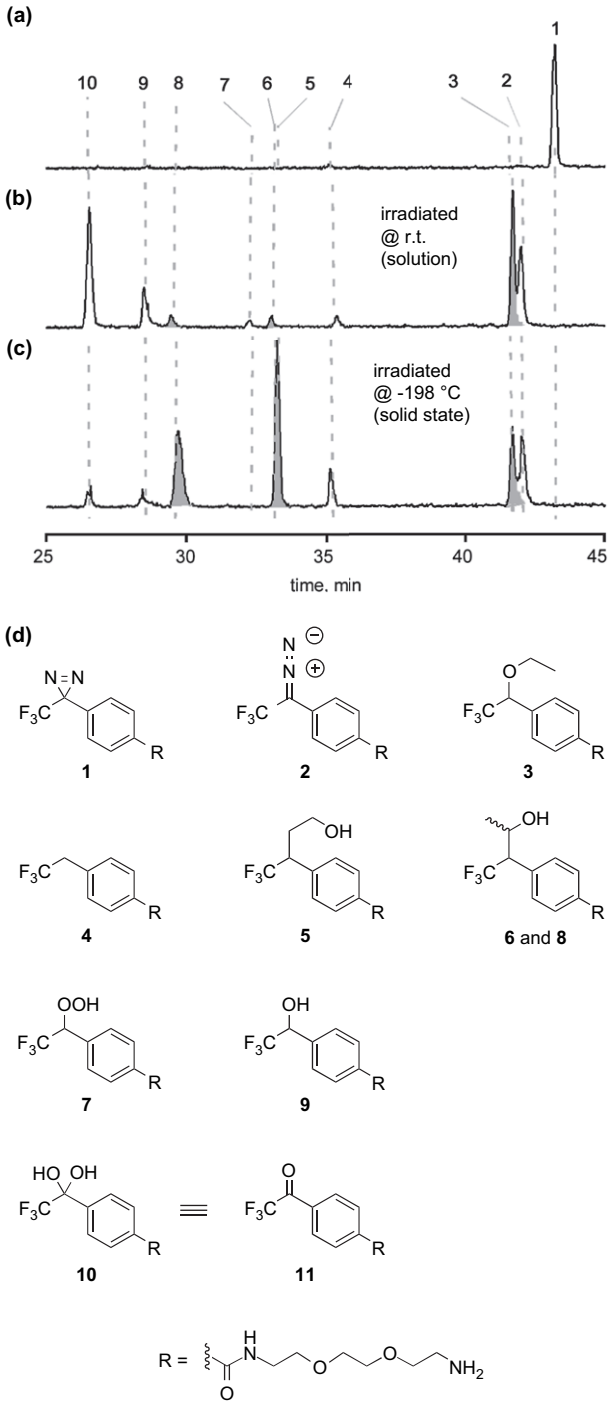

Figure 2. LC/ESI-MS chromatograms of **1** and the photolysis products in EtOH. The total ion chromatograms before photolysis (a) and after the photolysis of **1** performed at (b) room temperature and (c) −196 °C are shown; (d) structure of the photolysis products.

which does not have an ethoxy but rather a hydroxyethyl group (Fig. 3b and f). The presence of the hydroxyl group is responsible for the facile loss of HF in **5**, at least in part, since roughly 40% of the deuterium was lost in the MS/MS/MS spectrum of the deuteroxy analog of **5** (see Supplementary data, Fig. S1). Although the diastereomers **6** and **8** also have a hydroxyl group, the CID spectra of these compounds (Fig. 3c and d) were clearly different from the CID spectrum of **5** (Fig. 3b). In the CID spectra of **6** and **8**, secondary fragmentation channels, loss of 44 u from both *m*/*z* 274 and 231, were dominant. The loss of 44 u was shown to be attributable to C_2H_4O, which was originally in an ethanol molecule, but not including the hydrogen of the OH group (see Supplementary data, Figs. S2–S4). This observation implies that the hydrogen atom of the hydroxyl group specifically migrated to the ionic fragment as the neutral C_2H_4O was lost. Therefore, the characteristic product ions at *m*/*z* 230, 210, 187, and 167 can be regarded as a common feature of the cross-linked compounds having both 1-hydroxyalkyl and trifluoromethyl groups at the benzylic position. In other words, these ions may be useful for the LC/MS/MS-based characterization of the homologous products generated by the photo-cross-linking of **1** with other alcohols.

2.3. Reaction with other alcohols: LC/MS/MS-based characterization of the reaction products

We then performed photo-cross-linking experiments of **1** with PrOH, *i*-PrOH, BuOH, and *i*-BuOH in both liquid and solid states, and the resultant distributions of the photoadducts were analyzed. The total ion chromatograms and the MS/MS spectrum for each adduct (generated from the MS data sets for MH^+ at *m*/*z* 393 for propanols; MH^+ at *m*/*z* 407 for butanols) were obtained (Fig. 4), and their MS/MS fragmentation patterns were compared with those of the EtOH adducts (**3**, **5**, **6**, and **8**).

For example, the photo-cross-linking of **1** with *i*-PrOH in the solid state gave four isomeric products as expected, and all of them were separated by LC as shown in the chromatogram (Fig. 4a). The most hydrophobic isomer (**12**) gave a secondary fragmentation product with *m*/*z* 176 in its CID spectrum (Fig. 5a), and the presence of isopropyl ether was suggested. The ions at *m*/*z* 246 and 203 can be attributed to a loss of 42 u from *m*/*z* 288 and 245, respectively. These 42 u (C_3H_6: propene equivalent) losses are consistent with the presence of an isopropyl group. The second and third peaks in the chromatogram (**14**, **13**) showed secondary losses of HF and H_2O from *m*/*z* 245 in their CID spectra (Fig. 5b and c), and the presence of a 2-hydroxypropyl group at the benzylic position was suggested. The CID spectrum of the first peak (**15**) showed product ions at *m*/*z* 230, 210, 187, and 167, which are characteristic for a 1-hydroxyalkyl unit (i.e., 1-hydroxy-1,1-dimethyl group) at the benzyl position (Fig. 5d), as described previously.

The photo-cross-linking experiments of **1** with *i*-PrOH in the liquid state also gave four products, although the ratios between the products were quite different, i.e., the relative abundances of **13** and **14** were very low (Supplementary data, Fig. S5).

Similarly, the photo-cross-linking experiment of **1** with *i*-BuOH in the solid state gave the six expected isomeric products as shown in the chromatogram (Fig. 4b). The MS/MS spectrum of compound **16** showed characteristics of O–H insertion products, whereas the spectra of **17** and **21** clearly exhibited secondary fragment ions at *m*/*z* 230, 210, 187, and 167, revealing the presence of a pair of diastereomeric 1-hydroxyalkyl derivatives (Supplementary data, Fig. S6). Compounds **19** and **20** were suggested to be another diastereomeric pair containing a hydroxyalkyl side-chain since their MS/MS spectral patterns, including the secondary loss of H_2O, were almost identical. The remaining compound **18** may be assigned to the remaining isomer. The structures of **16**–**21** are summarized in Figure 6. Compounds **16**–**21** were also observed in the liquid state experiment but the relative abundances of the isomers were different from the solid state experiment. Again, the relative abundance of **16** was very high while the abundances of **19** and **20** were very low (Supplementary data, Fig. S5).

In the case of the photo-cross-linking experiment of **1** with PrOH in the solid state, six products were expected but only five peaks were observed in the chromatogram (Fig. 5c). We deduced all of the six expected isomers including two diastereomeric pairs were actually present but only five peaks were observed due to peak overlap. We assumed that each diastereomeric pair consisted

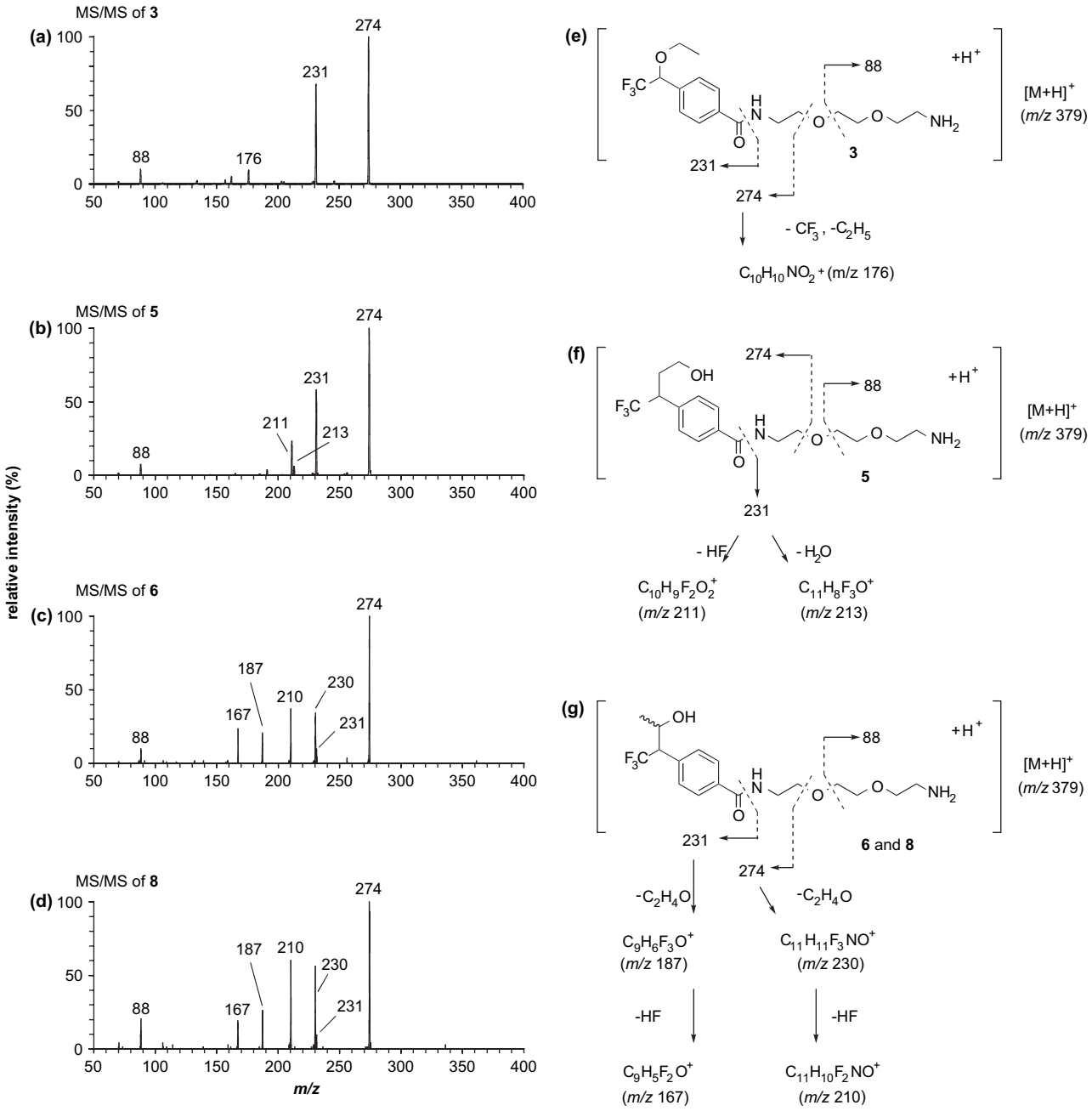

Figure 3. CID MS/MS spectra, chemical structure, and proposed fragmentation pathways of **3** (a and e), **5** (b and f), **6** (c and g), and **8** (d and g). These spectra were obtained by LC/MS/MS of the synthetic materials. The precursor ions at *m*/*z* 379 (protonated molecule of each compound) were converted to the product ions completely under the CID conditions used.

of roughly equal amounts of diastereomers, and that the two diastereomers in a pair were reasonably well separated by the LC system as in the previous cases. Based on these assumptions, the data could be interpreted as follows. The first and third peaks were assigned to the diastereomeric pair having a 1-hydroxyalkyl group at the benzylic position (**27** and **24**) as they showed almost identical MS/MS spectra containing *m*/*z* 230, 210, 187, and 167 ions (Supplementary data, Fig. S7). The last peak **22** was attributed to the O–H insertion product with *m*/*z* 176 in its MS/MS spectrum. The MS/MS spectra of the second and the fourth peak were similar, and both showed the characteristics of hydroxyalkyl derivatives. The synthetic 3-hydroxy-1-propyl derivative (**25**; see Supplementary data) eluted at the second peak position, and the MS/MS spectrum of the synthetic sample (Supplementary data, Fig. S8) was similar to that of the second peak. Therefore, the majority of the intensity of the second peak was considered to be due to **25**. The remaining fourth peak can be assigned to one of the 3-hydroxy-2-propyl derivatives (**23**); however, it is also very likely that a similar amount of diastereomer was present somewhere, as in the other cases. The second peak decreased to the size nearly equal to that of the fourth peak in the liquid state experiment (Supplementary data, Fig. S5). The MS/MS spectrum of the second peak in the liquid state products was similar to that of **23**. These observations suggested that most of the intensity of the second peak in the liquid state products was attributable to one of the 3-hydroxy-2-propyl derivatives (**26**). Hence, we concluded that the second peak in the solid state products was a mixture of **25** (major component) and **26** (minor component).

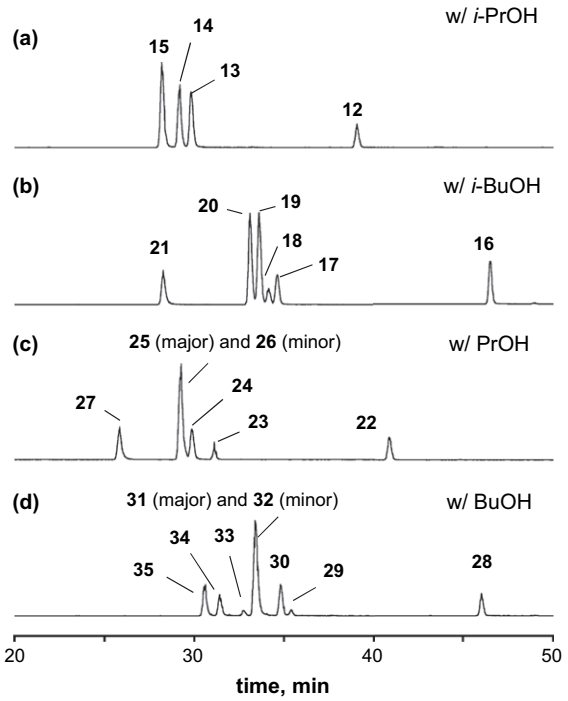

Figure 4. Total ion chromatograms for the photo-cross-linking products of **1** with *i*-PrOH (a), *i*-BuOH (b), PrOH (c), and BuOH (d) performed at −196 °C. As the chromatograms were obtained by LC/MS/MS analysis on the protonated molecules of each compound (*m*/*z* 393 for the chromatograms a and c; *m*/*z* 407 for b and d), only the photoadducts, which have those masses (i.e., isomeric products of carbene insertion into C–H or O–H) are present in each trace.

Similarly, only seven peaks were observed in the chromatogram of the photo-cross-linking of **1** with BuOH in the solid state (Fig. 4d), although eight isomeric products were expected. The first and fifth peaks were assigned to the diastereomeric 1-hydroxyalkyl derivatives (**35** and **30**) as they showed almost identical MS/MS spectra that included *m*/*z* 230, 210, 187, and 167 ions (Supplementary data, Fig. S9). The last peak was attributable to the O–H insertion product **28** because of *m*/*z* 176 in its MS/MS spectrum. The second, third, fourth, and sixth peaks gave MS/MS spectra having the characteristics of hydroxyalkyl derivatives. The third and sixth peaks showed similar peak areas, and their MS/MS spectra were similar to each other's as well. This suggested that the third and sixth peaks represent a pair of diastereomers. On the other hand, the synthetic 4-hydroxy-1-butyl derivative **31** eluted at the fourth peak position. The MS/MS spectra of the synthetic **31** (Supplementary data, Fig. S8) and the second and fourth peaks were similar to one another. We therefore concluded that another diastereomeric pair eluted in the second and fourth peaks, and the 4-hydroxy-1-butyl derivative **31** co-eluted with the fourth peak, which is significantly bigger than the second peak, since the second peak and the fourth peak showed similar peak areas in the chromatogram of the liquid state products. We assumed the amount, if any, of **31** in the liquid state products was very small. Unfortunately, we could not find any evidence to indicate that the diastereomeric pairs of **29** and **33** or of **32** and **34** correspond to the second and fourth peaks, or to the third and sixth peaks, respectively. Therefore, structural assignments for these diastereomeric pairs in Figure 6 may be reversed.

Based on the structural assignment discussed it was possible to categorize the cross-linked products into four classes (Fig. 7): (1) ether-type compounds that were generated by the insertion of the carbene into the O–H bonds highlighted in red; (2) compounds from the carbene insertion at C_1–H bonds highlighted in light blue; (3) compounds from the carbene insertion at the terminal methyl

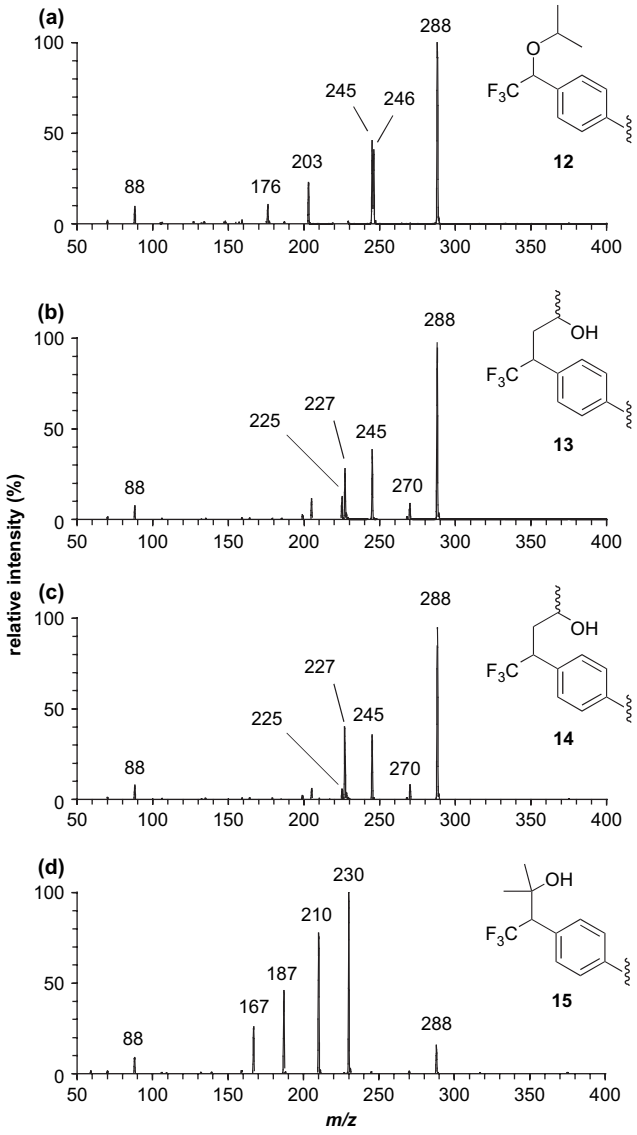

Figure 5. CID MS/MS spectra (LC/MS/MS) of the four isomeric photo-cross-linking products of **1** with *i*-PrOH. The precursor ions at *m*/*z* 393 (protonated molecule of each compound) were converted to the product ions completely under the CID conditions used.

C–H bonds highlighted in green; and (4) compounds from the carbene insertion at the internal methylene groups highlighted in purple. As described, we assigned two compounds that gave the same fragmentation pattern as a pair of diastereomers having the same atom connectivity in those cases where the reaction can produce a pair of diastereomers (such as **6** and **8**). In case one of the diastereomers overlapped with other products, the ratios of diastereomers having the same atom connectivity were estimated as 1:1 mixtures.

As can be clearly seen in Figure 7, all photolysis experiments performed in solution gave O–H insertion products in more than 70% of the total insertion reactions. It is generally accepted that alcohols in solution react with carbenes in the singlet state to give O–H insertion products as major products.[27] Interestingly, when a C–H bond into which the carbene inserts is on a methyl or methylene group, the level of C–H insertion products in solution tends to decrease as the C–H bond moves away from the hydroxyl group. On the other hand, insertions into the methine C–H bond in solution tend to dominate over those of other C–H bonds even when the methine C–H bond is away from the hydroxyl group. This

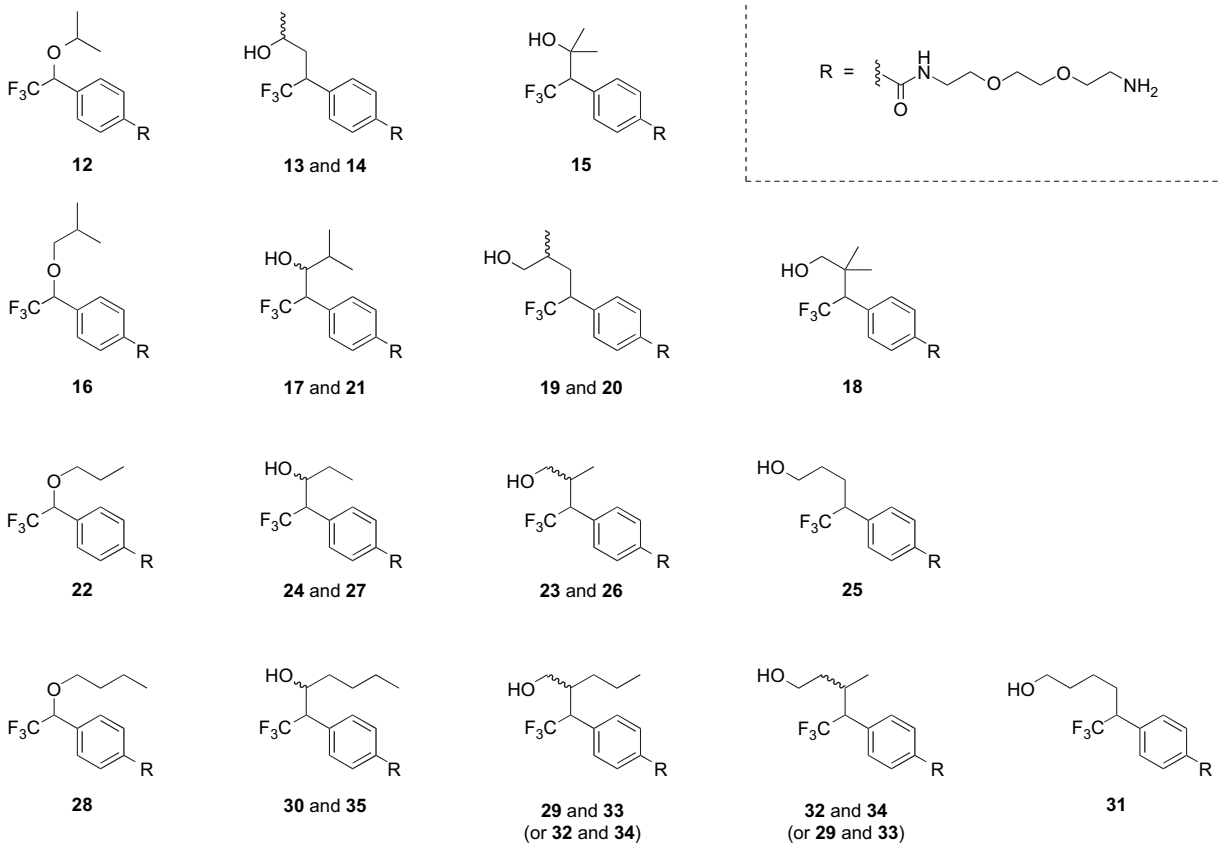

Figure 6. Summary of the structural assignments for the products of photo-cross-linking of **1** with *i*-PrOH, *i*-BuOH, PrOH, and BuOH.

tendency can be explained when the triplet carbene is thought of as an intermediate: the carbene's rate-limiting abstraction of a hydrogen atom produces a radical pair, both of which in turn bind to the formal insertion product.[16]

Solid-phase reactions are different from those occurring in solution in many respects. Striking differences were found in the percentage of terminal methyl C–H insertion products and O–H insertion products. In every case performed in the solid state, the percentage of total C–H insertions increased dramatically at the expense of O–H insertion reactions. In other words, the insertion reactions in the solid state became more nonselective. Furthermore, it should be noted that all possible isomers were produced under these conditions. Among the C–H insertion products, the percentage of C–H insertions at the terminal methyl groups was significantly increased.

3. Conclusion

In summary, we analyzed the photolysis products from **1** and five alcohols using LC/ESI-MS/MS and MS/MS/MS and found that the reactions in the solution phase were different from those in the solid phase. Especially in the solid phase, all C–H and O–H insertion products were formed in close to equivalent amounts. This observation is basically in accord with that of Tomioka et al., although they used other carbene species and alcohols that produced much simpler combinations of photo-cross-linked products.[22]

Although temperature effects should be considered for strict discussion, the results of this study support at least in part that the photo-cross-linking process for immobilizing small molecules on solid supports, in which solutions of small molecules were concentrated on the solid support in a solid or highly viscous state after which the small molecules were photo-cross-linked, takes place in a highly functional group-independent manner, which cannot be accomplished by conventional solution-phase reactions. Further evaluation of the nonselectiveness of the reaction of the carbene generated from **1** with other molecules will be reported in due course.

4. Experimental

4.1. Materials and methods

All chemicals and solvents were purchased from commercial vendors and used without further purification. *N*-[4-(3-Trifluoromethyl-3*H*-diazirin-3-yl)benzoyl]-2,2′-ethylenedioxybis-(ethylamine) (**1**) was prepared according to the reported procedure.[5]

4.2. Photolysis of 1 in alcoholic solution (general procedure)

An alcoholic solution of compound **1** (trifluoroacetic acid salt, 1 mg/mL, ~1 mL) in a 10 mL glass vial was exposed to UV irradiation of 4 J/cm^2 at 365 nm using a CL-1000L ultraviolet cross-linker (UVP Inc., CA, USA). The photolyzed solution was immediately stored at −20 °C until analyzed by LC/ESI-MS.

4.3. Photolysis of 1 in solidified alcohol at low temperature (general procedure)

An alcoholic solution of compound **1** (trifluoroacetic acid salt, 1 mg/mL, ~1 mL) in a 10 mL glass vial was cooled in a Dewar flask containing liquid N_2. The Dewar flask containing the solidified sample and liquid N_2 was set in a CL-1000L ultraviolet cross-linker and exposed to UV irradiation of 1 J/cm^2 at 365 nm. The surface of the sample became yellow. The sample was allowed to thaw, during which time the yellow color faded. The freeze–irradiation–thaw

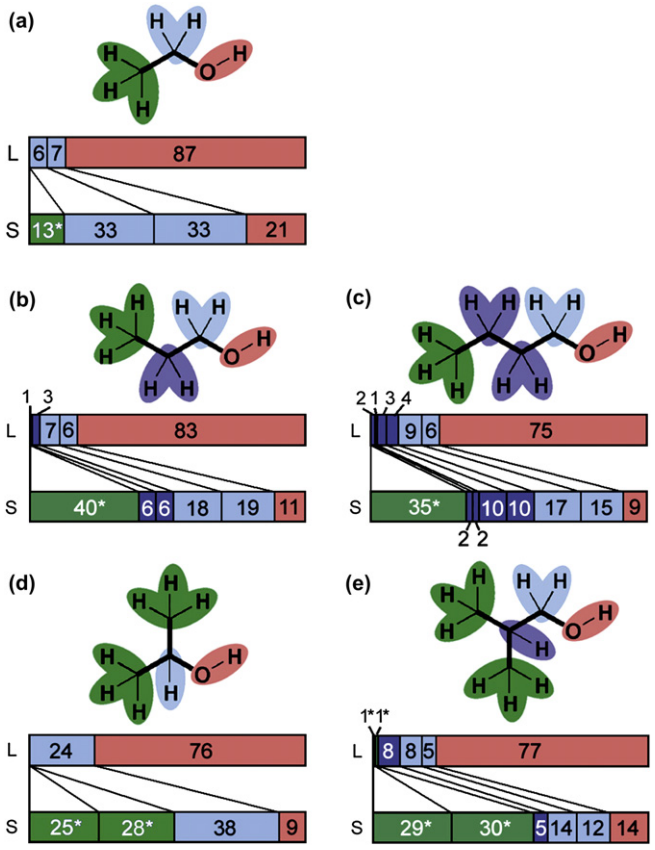

Figure 7. Distribution of C–H and O–H insertion products from the photolysis of **1** in alcohols. The reactions were performed at room temperature (liquid phase: designated as L) and at −196 °C (solid phase: S). Graphs and numerical values within or near each bar refer to the percentages of the products that were generated by the insertion of the carbenes into the chemical bonds shown in the same color. *Total percentage of C–H insertion product from three equivalent C–H bonds.

cycle was repeated another three more times. The photolyzed sample was stored at −20 °C until analyzed by LC/ESI-MS.

4.4. LC/MS and LC/MS/MS analyses of the photolysis products

The photolyzed solution was typically diluted 1/100 with water or 0.05% aq formic acid and analyzed with a 4000Q TRAP mass spectrometer (MSD Sciex, Foster City, CA, USA) equipped with an Agilent 1100 LC system using the following conditions.

Flow rate: 100 μl/min.
Solvent A: 0.05% formic acid in water (HPLC grade).
Solvent B: 0.05% formic acid in acetonitrile (HPLC grade).
Gradient: 5%B/0–5 min; 5–45%B/5–65 min; 45–80%B/65–70 min.
Column: Inertsil ODS-3 1.5 mm i.d.×200 mm (GL Science, Tokyo, Japan).
Column oven temperature: 25 °C.
Typical injection volume: 1 μL.
Ionization mode: ESI^+.
LC/MS scan mode: Q3.
LC/MS/MS scan mode: Triple Quadrupole (Q3 scan with Q1 precursor selection).
MS/MS (low-energy CID) condition: 45 V collision energy, N_2 collision gas.

In the typical LC/MS runs, MS/MS of selected precursor ions were also monitored. This facilitated matching of peaks between separate runs, even if there were some variations in retention time, which may be caused by a limited pumping reproducibility at the low-flow rate gradient.

Acknowledgements

The authors thank Ms. A. Asami for her technical support. This work was supported in part by the Daiichi Pharmaceutical Award in Synthetic Organic Chemistry; the Chemical Biology Project of RIKEN; grants from the MEXT, Japan; and a Grant-in-Aid for Scientific Research (C) (No. 17510187) from JSPS, Japan.

Supplementary data

Supplementary data associated with this article can be found in the online version, at doi:10.1016/j.tet.2008.04.031.

References and notes

1. Brunner, J. *Annu. Rev. Biochem.* **1993**, *62*, 483–514.
2. Richards, F. M.; Lamed, R.; Wynn, R.; Patel, D.; Olack, G. *Protein Sci.* **2000**, *9*, 2506–2517.
3. Craig, P. O.; Ureta, D. B.; Delfino, J. M. *Protein Sci.* **2002**, *11*, 1353–1366.
4. Gomez, G. E.; Cauerhff, A.; Craig, P. O.; Goldbaum, F. A.; Delfino, J. M. *Protein Sci.* **2006**, *15*, 744–752.
5. Kanoh, N.; Kumashiro, S.; Simizu, S.; Kondoh, Y.; Hatakeyama, S.; Tashiro, H.; Osada, H. *Angew. Chem., Int. Ed.* **2003**, *42*, 5584–5587.
6. Kanoh, N.; Kyo, M.; Inamori, K.; Ando, A.; Asami, A.; Osada, H. *Anal. Chem.* **2006**, *78*, 2463–2468.
7. Dilly, S. J.; Bell, M. J.; Clark, A. J.; Marsh, A.; Napier, R. M.; Sergeant, M. J.; Thompson, A. J.; Taylor, P. C. *Chem. Commun.* **2007**, 2808–2810.
8. Kanoh, N.; Asami, A.; Kawatani, M.; Honda, K.; Kumashiro, S.; Takayama, H.; Simizu, S.; Amemiya, T.; Kondoh, Y.; Hatakeyama, S.; Tsuganezawa, K.; Utata, R.; Tanaka, A.; Yokoyama, S.; Tashiro, H.; Osada, H. *Chem. Asian J.* **2006**, *1*, 789–797.
9. Kanoh, N.; Honda, K.; Simizu, S.; Muroi, M.; Osada, H. *Angew. Chem., Int. Ed.* **2005**, *44*, 3559–3562.
10. Kuramochi, K.; Haruyama, T.; Takeuchi, R.; Sunoki, T.; Watanabe, M.; Oshige, M.; Kobayashi, S.; Sakaguchi, K.; Sugawara, F. *Bioconjugate Chem.* **2005**, *16*, 97–104.
11. Choi, J. W.; Chen, J.; Schreiber, S. L.; Clardy, J. *Science* **1996**, *273*, 239–242.
12. Ki, S. W.; Ishigami, K.; Kitahara, T.; Kasahara, K.; Yoshida, M.; Horinouchi, S. *J. Biol. Chem.* **2000**, *275*, 39231–39236.
13. Importance of high reactivity and low functional group selectivity of the photogenerated carbenes as small molecule capturing agents have been discussed earlier. See Refs. 5 and 8.
14. Quite recently, Schreiber and Koehler et al. reported a new capture strategy that allows immobilization of common reactive functional groups present in both synthetic and natural compounds. See: (a) Bradner, J. E.; McPherson, O. M.; Mazitschek, R.; Barnes-Seeman, D.; Shen, J. P.; Dhaliwal, J.; Stevenson, K. E.; Duffner, J. L.; Park, S. B.; Neuberg, D. S.; Nghiem, P.; Schreiber, S. L.; Koehler, A. N. *Chem. Biol.* **2006**, *13*, 493–504; (b) Bradner, J. E.; McPherson, O. M.; Koehler, A. N. *Nat. Protocol* **2006**, *1*, 2344–2352; (c) Schmitz, K.; Haggarty, S. J.; McPherson, O. M.; Clardy, J.; Koehler, A. N. *J. Am. Chem. Soc.* **2007**, *129*, 11346–11347.
15. Platz, M. S. *Kinetics and Spectroscopy of Carbenes and Biradicals*; Platz, M. S., Ed.; Plenum: New York, NY, 1990; pp 143–212.
16. Tomioka, H. *Res. Chem. Intermed.* **1994**, *20*, 605–634.
17. Gupta, C. M.; Costello, C. E.; Khorana, H. G. *Proc. Natl. Acad. Sci. U.S.A.* **1979**, *76*, 3139–3143.
18. Brunner, J.; Senn, H.; Richards, F. M. *J. Biol. Chem.* **1980**, *255*, 3313–3318.
19. Nassal, M. *J. Am. Chem. Soc.* **1984**, *106*, 7540–7545.
20. Platz, M.; Admasu, A. S.; Kwiatkowski, S.; Crocker, P. J.; Imai, N.; Watt, D. S. *Bioconjugate Chem.* **1991**, *2*, 337–341.
21. Delfino, J. M.; Schreiber, S. L.; Richards, F. M. *J. Am. Chem. Soc.* **1993**, *115*, 3458–3474.
22. Tomioka, H.; Suzuki, S.; Izawa, Y. *J. Am. Chem. Soc.* **1982**, *104*, 3156–3162.
23. The structures of these compounds were determined by comparison with authentic synthetic samples. See Supplementary data.
24. Diderich, G. *Helv. Chim. Acta* **1972**, *55*, 2103–2111.
25. Bethell, D.; Stevens, G.; Tickle, P. *J. Chem. Soc. D* **1970**, 792–794.
26. Production of **5** was below the detection limit in this case.
27. Closs, G. L.; Rabinow, B. E. *J. Am. Chem. Soc.* **1976**, *98*, 8190–8198.